

Electron-distribution-function cutoff mechanism in a low-pressure afterglow plasma

Robert R. Arslanbekov and Anatoly A. Kudryavtsev

Institute of Physics, St. Petersburg State University, St. Petersburg, 198904, Russia

Lev D. Tsendin

Physical Technical Department, St. Petersburg State Technical University, St. Petersburg, 195251, Russia

(Received 7 February 2001; published 13 June 2001)

A model is developed for self-consistent simulations of transient phenomena in a low-pressure afterglow plasma. The model is based on the nonlocal approach which allows a kinetic description of the plasma decay under nonquasistationary conditions. Such conditions arise when collisions (mainly electron-electron) are not sufficient for the electron distribution function (EDF) to follow changes in the self-consistent electric fields and the ion density once the power is turned off. As a result, collisions cannot provide the electron and ion particle balance by allowing electrons to flow out of the potential well. A cutoff mechanism is suggested that provides such a balance during the transient period—from the glow, stationary plasma to the quasistationary, afterglow plasma. This mechanism is essential for determining correctly the self-consistent wall potential (and hence the energy of ions impinging upon the wall surface) and other parameters, such as diffusion cooling, which is the most important cooling mechanism at low pressures. These phenomena are modeled using the time-dependent nonlocal electron Boltzmann equation with a nonlinear electron-electron collision operator. A numerical treatment is made by extending Rockwood's method for finite-difference discretization of this operator in the total energy formulation. The model calculates self-consistently the temporal evolution of the nonlocal EDF and the electric potentials in the plasma and the wall sheath. Strongly non-Maxwellian EDF's are predicted and it is observed that, depending on plasma conditions, the transient period maybe rather long, of order of the ambipolar diffusion time, lower pressures resulting in longer transient times. The proposed approach can be applied to model self-consistently pulsed plasmas during both the power-on and power-off periods, including the breakdown period.

DOI: 10.1103/PhysRevE.64.016401

PACS number(s): 52.80.-s, 52.65.-y, 52.25.Dg

I. INTRODUCTION

The afterglow (postdischarge) plasma has attracted much attention in the past several decades. The recently increased interest came about as a result of development of advanced, pulsed plasma sources operating at low pressures. Much effort has been invested in comprehensive experimental investigation and theoretical modeling of such plasmas (e.g., [1]). The global (e.g., [1]) and fluid (e.g., [2]) models have been most commonly used to describe power-modulated plasmas. Simulations using the particle-in-cell with Monte Carlo collisions (PIC-MCC) codes have also been reported (e.g., [3,4]).

Since at low pressures the electron kinetics is essentially nonlocal and the electron distribution function (EDF) is likely to be non-Maxwellian, the global and fluid models may fail to predict the plasma decay correctly, especially in the early afterglow (e.g., [5]). A kinetic treatment is therefore necessary, taking into account the EDF nonlocality. Such a treatment can be naturally performed using the PIC-MCC codes. The PIC-MCC methods, however, are computationally costly and become even more so if electron-electron ($e-e$) collisions are taken into account at considerable electron densities ($n_e \gtrsim 10^{10} \text{ cm}^{-3}$). As such, low plasma densities are treated ($n_e \lesssim 10^8 - 10^9 \text{ cm}^{-3}$ [3,4]) and $e-e$ collisions are generally neglected in the PIC-MCC simulations. Since $e-e$ collisions are essential in describing an afterglow plasma (e.g., Maxwellization), they need to be included and treated appropriately. Therefore, since the global and fluid models

are largely oversimplistic and the direct PIC-MCC methods are computationally demanding, the appropriate approach is to use the electron kinetic equation. However, the solution of the time- and space-dependent kinetic equation with self-consistent electric fields is a complicated task. In the present paper, we employ simplifications based on the nonlocal approach proposed by Bernstein and Holstein [6] and by Tsendin [7]. The correctness and effectiveness of this approach has been demonstrated for various types of plasma discharge in the active phase (power-on period); to cite just a few examples, in Ref. [8] for an inductively coupled plasma (ICP), in Ref. [9] for a positive column plasma (PCP), and in Ref. [10] for a capacitively coupled plasma (CCP).

In Ref. [5], a semianalytic method based on the nonlocal approach was proposed for self-consistent modeling of a low-pressure afterglow plasma under nonlocal conditions. The method consists in solving simplified, nonlocal kinetic equations coupled with particle- and energy-balance equations. The applicability of this method was validated by numerical solution of the full time- and space-dependent kinetic equation. The main assumption of this method is that the EDF is quasistationary. This assumption is valid provided that collisions (mainly $e-e$, frequency ν_e) are frequent enough for the EDF to adjust itself to changes in the self-consistent electric potential. Such changes take place on a time scale of order of the ambipolar diffusion time τ_{amb} and the assumption of the EDF quasistationarity turns out to be valid at moderately low pressures. With further decrease of pressure, the following phenomena can become manifest. It

was demonstrated in Ref. [5] that the particle and energy balances are provided by particle and energy fluxes (in energy space) out of the potential well (which is determined by the wall potential energy $e\Phi_w$), the characteristic time of electron escape matching the time of ion ambipolar diffusion to the wall, τ_{amb} . These (positive) fluxes in their turn *can exist only due to e - e collisions* which enable electrons to escape from the potential well. Any other type of collision (inelastic, quasielastic, etc.) cannot generate such fluxes, since collisions other than e - e collisions result in fluxes of electrons toward low energies (negative fluxes). Clearly, during the power-on period, these outflows of electrons are due to the electric field sustaining the plasma (e - e collisions being generally negligible), which accelerates the electrons, allowing them to escape from the potential well. But once the input power has been turned off, an interesting situation is realized. Typically, the wall potential energy $e\Phi_w$ is high ($e\Phi_w \gtrsim \epsilon_i$, where ϵ_i is the ionization potential; i.e., $e\Phi_w \gtrsim 20$ eV for rare gases, such as He and Ar) during the power-on period. As such, the frequency of e - e collisions at these high energies is low (provided that the electron density is not very high), namely, $\nu_e(e\Phi_w) < \tau_{amb}^{-1}$, and hence e - e collisions cannot provide (positive) particle fluxes out of the potential well. Under these circumstances, the wall potential has to start to decrease fast enough in order to let electrons leave the potential well and escape quickly to the wall. Such a fast decrease of $e\Phi_w$ causes portions of the EDF with energies close to $e\Phi_w$ to be effectively cut off from the bulk EDF, this representing the “cutoff” mechanism. The particle loss due to the cutoff mechanism is accompanied by an energy loss which can be identified with a modified diffusion cooling mechanism—the most important cooling mechanism at low pressures.

The importance of the mechanisms described is evident for predicting correctly, among other things, the energy of various ion species impacting on a wall surface or on a solid object (such as a wafer) immersed in the plasma. Comprehensive modeling can aid the development of methods of control over charged-species fluxes, which is one of the ultimate goals of low-pressure plasma processing. In this complementary paper we extend the model proposed in Ref. [5] by focusing attention mainly on the transient phenomena. The paper is organized as follows. In Sec. II, the assumptions and description of the physical model are given. In Sec. II A, the nonlocal electron Boltzmann equation is presented, together with the e - e collision operator. The particle- and energy-balance equations are analyzed in Sec. II B. The numerical scheme is detailed in Sec. III, and the simulation results and their discussion are given in Sec. IV. Finally, the summary and conclusions are outlined in Sec. V.

II. PHYSICAL MODEL

The plasma we are interested in is an afterglow plasma. The gas pressure p is considered to be low so that the electron energy relaxation length λ_e is larger than the characteristic discharge chamber dimension Λ , i.e., $\lambda_e > \Lambda$. A mainly collisional regime for electrons is considered, in which the electron mean free path in collisions with atoms, λ (fre-

quency ν), is smaller than Λ , i.e., $\lambda \lesssim \Lambda$; however, there are no limitations in principle for the model to be valid in a collisionless regime. The model gas is a noble gas, Ar. We adopt a one-dimensional cylindrical geometry, with the tube radius being R (so that $\Lambda \approx R/2.4$). The analysis, however, can be extended to a multidimensional case (e.g., [8]) since the employed nonlocal kinetic equation in terms of the total energy ϵ does not depend explicitly on geometry. We do not specify the type of plasma generation in the active phase (power-on period). It can be an ICP, CCP, or PCP. The type of discharge can be specified by discharge conditions (geometry, gas pressure) and by the initial EDF (electron density, mean energy, etc.). Here we study the plasma decay from the moment when the power has been switched off. Hence, we assume that at time $t=0$ there is no power going into the gas and there are no currents in the external circuit. However, since the typical time scale of the mechanisms studied here is of order of a few tens of microseconds, a finite power fall time of a few microseconds can exist. We also assume that all high-voltage sheaths, which may be present in the active phase (e.g., in a CCP), have collapsed in a short time (of order of the ion transit time across the sheath) and the plasma consists only of a quasineutral region and narrow (few Debye radii) space-charge wall sheaths. In the quasineutral region, the space-charge (ambipolar) potential $\Phi(r)$ dominates and $n = n_i = n_e$ [where n is the plasma density and $n_e(n_i)$ is the electron (ion) density]. In the wall sheaths, a steep change (jump) $\Delta\Phi_w$ in potential takes place, which is necessary to confine most of the electrons and to balance total electron and ion currents to the (dielectric or conducting) wall, the total wall potential being $\Phi_w = \Phi(R) + \Delta\Phi_w$. Spatially resolving the narrow (mainly collisionless for both electrons and ions) wall sheaths can be avoided by choosing appropriate boundary conditions at the wall. Since the plasma studied is nonstationary, all plasma quantities are allowed to vary in time and so have explicit time dependence, such as $\Phi = \Phi(t, r)$, $\Phi_w = \Phi_w(t)$, the EDF $f_0 = f_0(t, \epsilon)$, etc.; for convenience, the argument t will be dropped in most of the following formulas.

A. Nonlocal electron Boltzmann equation

Generally, in order to find the EDF, a nonlinear (integro-differential) time- and space-dependent kinetic equation has to be solved, which is a computer intensive task, especially in a self-consistent problem. In Ref. [5], we solved such a full kinetic equation and compared the results with solutions of a simplified nonlocal kinetic equation under the assumption of EDF quasistationarity. Here we cannot make such an assumption and hence use the nonlocal electron Boltzmann equation directly.

At low pressures, the key simplification is to use the nonlocal approach (see Refs. [7,11,12] for details). This approach can be applied provided that $\lambda_e > \Lambda$. In the elastic energy range ($w < w^*$) $\lambda_e \approx \lambda \sqrt{\nu/(\nu_e + \delta\nu)}$ (for Maxwellian electrons, $\lambda_e \approx \lambda/\sqrt{\delta}$) and in the inelastic energy range ($w > w^*$) $\lambda_e \approx \sqrt{\lambda\lambda^*/3}$ (for small ν_e), where $\delta = 2m/M$ is the fraction of electron energy lost in a single quasielastic electron-atom (e - a) collision and $\lambda^* = \nu/\nu^*$ and ν^* are, re-

spectively, the mean free path and frequency of inelastic e - a collisions. Estimations show that for Ar in the energy range of interest nonlocal conditions with $\lambda_e > \Lambda$ occur when the gas pressure is lower than a few Torr (for a 1-cm-radius discharge). Under nonlocal conditions, electrons transit radially without significant changes in the so-called total energy $\epsilon = w + e\Phi(r)$ (here, the electron charge $e < 0$ and $\Phi < 0$, so that $e\Phi > 0$), which becomes an approximate constant of motion and is hence a convenient independent variable to replace the kinetic energy $w = \frac{1}{2}mv^2$. Two groups of electrons can be distinguished, namely, trapped ($\epsilon \leq e\Phi_w$) and free ($\epsilon > e\Phi_w$) electrons. A trapped electron with a total energy ϵ can only move within an accessible region determined by $\epsilon \leq e\Phi(r)$ or $r \leq r^*(\epsilon)$, and a free electron quickly escapes to the wall by free diffusion (collisional regime, $\lambda < \Lambda$) and by scattering into the wall loss cone (collisionless regime, $\lambda > \Lambda$).

The nonlocal kinetic equation applies strictly only for the trapped electrons. The approach, however, can be extended, and the free electrons can also be described by the same equation by introducing a wall loss term with a characteristic wall loss time

$$\tau_w = \frac{\Lambda^2}{D_r} + \frac{1}{2} \left(\frac{R + \lambda}{\lambda} \right) \frac{4\pi}{\delta\Omega} \frac{1}{\nu}, \quad (1)$$

where $D_r = \frac{1}{3}\lambda^2\nu$ is the electron free-diffusion coefficient and $\delta\Omega \approx 2\pi[1 - \sqrt{(e\Phi_w - e\Phi)/(\epsilon - e\Phi)}]$ is the wall loss cone; this approach is valid for $\delta\Omega \ll 4\pi$, namely, for ‘‘almost trapped’’ electrons. In Ref. [9], by carrying out a detailed comparison with Monte Carlo calculations, this approach was shown to be appropriate in a large electron energy range of up to 100 eV for a dc positive column plasma. Not only in the collisional regime ($\lambda \leq \Lambda$ and $\lambda_e > \Lambda$) does this approach work, but also, surprisingly, in the (near) collisionless regime ($\lambda \gtrsim \Lambda$; see Ref. [13] for details), where a significant anisotropy of the EDF is manifest and hence the two-term spherical harmonic approximation is strictly not valid. It can be expected that this approach will be valid also for a nonstationary afterglow plasma since the time of free radial diffusion/transit $\tau_f \sim \Lambda^2/D_r + R/\nu$ is fast compared with the slow time of variation of the ambipolar (Φ) and wall (Φ_w) potentials. However, since the nonlocal kinetics is obtained by averaging over electrons’ radial transits, phenomena occurring on a time scale faster than τ_f (typically, $\tau_f \leq 0.1$ – $1 \mu\text{s}$ at low pressures) cannot be adequately described.

Thus, we can write the nonlocal kinetic equation for the EDF $f_0(t, \epsilon)$ as

$$\frac{\partial f_0}{\partial t} + \frac{\mathcal{V}_\Phi}{\sqrt{w}} \frac{\partial f_0}{\partial \epsilon} = \frac{1}{\sqrt{w}} \frac{\partial}{\partial \epsilon} \sqrt{w} J_{ee} - \frac{f_0}{\tau_w}, \quad (2)$$

where a spatially averaged quantity in cylindrical geometry is

$$\bar{X}(\epsilon) = \frac{1}{R^2/2} \int_0^{r^*(\epsilon)} X(\epsilon, r) r dr, \quad (3)$$

and the time dependence is assumed (argument t dropped) for all quantities: $w = w(t, \epsilon, r) = \epsilon - e\Phi(t, r)$, $\sqrt{w} = \sqrt{w}(t, \epsilon)$, etc. Note that τ_w has implicit time dependence via mainly the dependence $\delta\Omega = \delta\Omega[e\Phi_w(t)]$. Since the ambipolar potential Φ in the definition of the total energy ϵ is time dependent, there is an additional term in the time derivative of the EDF f_0 in Eq. (2) (see, e.g., Ref. [14]) with

$$\overline{\mathcal{V}_\Phi} = e \sqrt{w} \frac{\partial \Phi}{\partial t}. \quad (4)$$

Here, $\mathcal{V}_\Phi = \mathcal{V}_\Phi(t, \epsilon)$ and $\mathcal{V}_\Phi/\sqrt{w} \sim e \partial \Phi / \partial t$, and so this term is generally small compared with the collision term: $|e \partial \Phi / \partial t| \ll w \nu_e$ [see also the discussion of Eq. (10) below].

After some manipulations, the nonlinear e - e collision operator in total-energy (spatially averaged) formulation can be written as

$$\overline{\sqrt{w} J_{ee}} \equiv \mathcal{J}_{ee} = \mathcal{V}_e f_0 + \mathcal{D}_e \frac{\partial f_0}{\partial \epsilon}, \quad (5)$$

with the e - e dynamic friction and diffusion coefficients, respectively,

$$\mathcal{V}_e = \nu_{e0} \int_0^{\epsilon} \overline{w^{1/2}(\epsilon')} f_0(\epsilon') d\epsilon', \quad (6a)$$

$$\mathcal{D}_e = \nu_{e0} \frac{2}{3} \left(\int_0^{\epsilon} \overline{w^{3/2}(\epsilon')} f_0(\epsilon') d\epsilon' + \overline{w^{3/2}(\epsilon)} \int_{\epsilon}^{\infty} f_0(\epsilon') d\epsilon' \right), \quad (6b)$$

where $\nu_e = \nu_{e0} n_e / w^{3/2}$ is the e - e collision frequency with $\nu_{e0} = 2\sqrt{2}\pi e^4 \ln \Lambda / \sqrt{m_e}$. It can be seen that the e - e collision operator in kinetic energy formulation (e.g., [12,5]) and that of Eqs. (5) and (6) in total-energy (spatially averaged) formulation have similar forms with the following substitutions: $w \rightarrow \epsilon$, $w^{1/2} \rightarrow \overline{w^{1/2}}$, and $w^{3/2} \rightarrow \overline{w^{3/2}}$. The e - e collision operator in Eq. (5) can be shown (after multiplying it by $\overline{w^{1/2}}$ and $\epsilon \overline{w^{1/2}}$ and then integrating over total energy) to conserve the volume-averaged density and mean total (not kinetic) energy, which implies that

$$\int_0^{\infty} \frac{\partial \mathcal{J}_{ee}}{\partial \epsilon} d\epsilon = 0 \quad \text{and} \quad \int_0^{\infty} \epsilon \frac{\partial \mathcal{J}_{ee}}{\partial \epsilon} d\epsilon = 0. \quad (7)$$

In Eq. (2) we have neglected quasielastic (frequency $\delta\nu$) and inelastic (frequency ν^*) e - a collisions. These collisions can be treated in a straightforward manner (e.g., [7,12,9]): quasielastic collisions can be cast into the Fokker-Planck form of Eq. (5) and for inelastic collisions only loss terms proportional to νf_0 need be retained. For simplicity these types of collision are neglected here. This is reasonable for quasielastic collisions since at low pressures $\delta\nu \ll \nu_e$ in the energy range of interest. Inelastic collisions in their turn are not important when the wall potential (above which the EDF falls off rapidly) does not significantly exceed w^* , which is the case under the conditions studied. It turns out that, for the physical mechanisms presently investigated, both elastic and

inelastic collisions are nonessential (in fact, such collisions can even enhance these mechanisms) and their possible impact will be discussed in Sec. IV.

From the EDF $f_0(\epsilon)$, the electron density n_e can be calculated as

$$n_e(r) = \int_{e\Phi(r)}^{\infty} \sqrt{\epsilon - e\Phi(r)} f_0(\epsilon) d\epsilon, \quad (8)$$

and so can the mean kinetic energy $W_e(r) = \int_{e\Phi(r)}^{\infty} \epsilon w^{3/2} f_0 d\epsilon / n_e$. In the case of the Maxwell-Boltzmann EDF

$$f_M = \frac{2}{\sqrt{\pi}} \frac{n_{e0}}{T_e^{3/2}} \exp(-\epsilon/T_e), \quad (9)$$

where n_{e0} is the central electron density (at the location of $\Phi=0$), an electron temperature $T_e = \frac{2}{3} W_e$ can be introduced.

B. Electron density and mean total energy-balance equations

In this section, we derive and analyze the particle- and energy-balance equations. It can be argued that since we solve the kinetic equation there is no need to derive the balance equations. Nonetheless, in order to gain insight into the governing mechanisms, it is instructive to consider and analyze these equations; moreover, the particle-balance equation will be necessary to calculate the wall potential. Since under nonlocal conditions two distinct, almost independent groups of electrons (namely, trapped and free) exist, it is more appropriate physically to analyze the corresponding balance equations for the trapped electrons, those for all electrons ($\epsilon \in [0, \infty]$) being unhelpful (e.g., in the energy balance of all electrons, e - e collisions are absent, which can lead to incorrect results; see Ref. [15]).

Before proceeding with the mathematical treatment, let us consider the physical picture. Under nonlocal conditions, the trapped electrons represent a ‘‘reservoir’’ (formed by the potential well) of particles and energy. As the plasma decays, particle and energy fluxes (in energy space) flow out of this reservoir via an ‘‘orifice’’ at $\epsilon = e\Phi_w$. Once these fluxes in energy space have left the potential well, they quickly transform into fluxes in configuration space (see Ref. [5]; see also Ref. [15]). The particle flux out of the potential well is necessary in order to balance the ion flux in the plasma and at the wall. Those electrons with energies close to the potential well energy (orifice) can gain energy in collisions with other electrons and thereby escape out. (Note that e - a collisions, which were neglected here, cannot result in particle outflows; see also the discussion in Sec. IV.) If, however, the frequency of e - e collisions is not high enough (which is likely the case at high energies), the (energy) level of this orifice will have to be lowered gradually to let the electrons leave the reservoir. This is the essence of the cutoff mechanism when the trapping potential energy decreases fast enough, effectively cutting off high-energy electrons from the bulk, trapped EDF (which itself does not have time to react to such changes). These electrons become free and thus carry the electron current. Associated with this particle loss induced

by the cutoff mechanism is an energy loss representing a cooling mechanism for the trapped electrons.

The mathematical treatment proceeds by multiplying the nonlocal kinetic equation (2) by $w^{1/2}$ and $\epsilon w^{1/2}$ and then integrating over total energy from 0 to $e\Phi_w$. It should be pointed out that the first moment of the nonlocal kinetic equation gives the evolution of the mean total energy (its volume-averaged value), not the kinetic one. This is physically clear and, as a consequence, the e - e collision operator conserves the mean total (not kinetic) energy [see Eq. (7)]. Hereinafter, we denote quantities related to trapped electrons by careted variables (such as \hat{n}_e , etc.) and volume-averaged quantities by $\langle \dots \rangle$, where $\langle X \rangle = 2 \int_0^R X(r) r dr / R^2$. The particle-balance equation for the volume-averaged density of trapped electrons, $\langle \hat{n}_e \rangle = \int_0^{e\Phi_w} \sqrt{w} f_0 d\epsilon$, then reads as

$$\frac{d\langle \hat{n}_e \rangle}{dt} = \hat{\mathcal{I}}_{\Phi}(t) - \hat{\mathcal{I}}_e(t) - \hat{\mathcal{I}}_{\text{co}}(t), \quad (10)$$

where $\hat{\mathcal{I}}_e = \mathcal{J}_{ee}(\epsilon = e\Phi_w)$ is the particle flux out of the potential well due to e - e collisions ($\hat{\mathcal{I}}_e \propto \nu_e$) and

$$\hat{\mathcal{I}}_{\Phi} = -\mathcal{V}_{\Phi} f_0|_{\epsilon=e\Phi_w} \quad \text{and} \quad \hat{\mathcal{I}}_{\text{co}} = -\sqrt{w} f_0|_{\epsilon=e\Phi_w} \frac{de\Phi_w}{dt}. \quad (11)$$

Here, $\hat{\mathcal{I}}_{\Phi}$ is due to time varying Φ : $\mathcal{I}_{\Phi} \propto \partial\Phi/\partial t > 0$. The third term $\hat{\mathcal{I}}_{\text{co}}$ on the right-hand side (rhs) of Eq. (10) represents a particle loss due to the cutoff mechanism, proportional to the $e\Phi_w$ decay rate and the EDF amplitude at $\epsilon = e\Phi_w$. (Note that $\hat{\mathcal{I}}_e$ is mainly determined by the slope of the EDF at $\epsilon = e\Phi_w$.) Clearly, since the wall potential varies with time much faster than the ambipolar potential does (i.e., $|d\langle\Phi\rangle/dt| \sim |d\langle W_e\rangle/dt| \ll |d\Phi_w/dt|$), typically, $\hat{\mathcal{I}}_{\Phi} \ll \hat{\mathcal{I}}_{\text{co}}$.

Analogously, the balance equation for the (volume-averaged) mean total energy of trapped electrons, $\hat{\mathcal{E}}_e = \int_0^{e\Phi_w} \epsilon \sqrt{w} f_0 d\epsilon$, reads as

$$\frac{d\hat{\mathcal{E}}_e}{dt} = \hat{\mathcal{H}}_{\Phi}(t) - \hat{\mathcal{H}}_e(t) - \hat{\mathcal{H}}_{\text{co}}(t), \quad (12)$$

where $\hat{\mathcal{H}}_{\Phi} = e\Phi_w \hat{\mathcal{I}}_{\Phi} + \int_0^{e\Phi_w} \epsilon w f_0 \mathcal{V}_{\Phi} d\epsilon$ is due to the same mechanism as $\hat{\mathcal{I}}_{\Phi}$, i.e., $\hat{\mathcal{H}}_{\Phi} \propto \partial\Phi/\partial t$; $\hat{\mathcal{H}}_e = e\Phi_w \hat{\mathcal{I}}_e$ is the energy flux out of the potential well due to e - e collisions; and $\hat{\mathcal{H}}_{\text{co}} = e\Phi_w \hat{\mathcal{I}}_{\text{co}}$ stands for an energy loss due to the cutoff mechanism. Typically, as is the case in the particle balance, $\hat{\mathcal{H}}_{\Phi} \ll \hat{\mathcal{H}}_{\text{co}}$. In Eq. (12), we have neglected the term representing cooling in collisions with free electrons, $\hat{\mathcal{H}}_f = \int_{e\Phi_w}^{\infty} \mathcal{J}_{ee} d\epsilon$, since the number of free electrons is small (see Ref. [5]). However, in a late afterglow, when $T_e < 0.1$ – 0.3 eV, $\hat{\mathcal{H}}_f$ can represent an efficient *heating* mechanism in collisions with superthermal electrons ($w \gg T_e$) produced in reactions with participation of metastable atoms [16] (see also Ref. [15]).

It is clear that the cooling mechanisms $\hat{\mathcal{H}}_e$ and $\hat{\mathcal{H}}_{co}$ accompany the particle losses due to e - e collisions and the cutoff mechanism, respectively. In a quasistationary plasma, the particle outflow due to e - e collisions was associated with diffusion cooling [5]—the most important cooling mechanism (with a rate larger than the cooling rate in e - a collisions) at low pressures. Here, however, an additional particle and energy loss mechanism emerges, and the diffusion cooling can be identified with the sum of these two cooling mechanisms, $\hat{\mathcal{H}}_e + \hat{\mathcal{H}}_{co} = e\Phi_w(\hat{\mathcal{I}}_e + \hat{\mathcal{I}}_{co}) \approx e\Phi_w \mathcal{I}_w$ (see below).

Finally, with the particle-balance equation (10) for $\langle \hat{n}_e \rangle$ being derived and with a given EDF $f_0(\epsilon)$ [calculated from Eq. (2)], it is possible to find the decay rate of $\langle n_e \rangle$, which will be needed to derive an equation for Φ_w (see Sec. II D). However, it appears that for this purpose it is more appropriate numerically to use the particle-balance equation of all electrons directly, which yields in its turn

$$\frac{d\langle n_e \rangle}{dt} = -\mathcal{I}_w(t) = - \int_{e\Phi_w}^{\infty} \frac{f_0}{\sqrt{w} \tau_w} d\epsilon, \quad (13)$$

with \mathcal{I}_w representing the flux of free electrons to the wall. Clearly, $n_e \approx \hat{n}_e$, the number of free electrons being small. Moreover, $\mathcal{I}_w \approx \hat{\mathcal{I}}_e + \hat{\mathcal{I}}_{co}$, which means that the ‘‘source’’ of free electrons is (trapped) electrons escaped from the potential well and which also establishes a connection between the fluxes in energy space (i.e., $\hat{\mathcal{I}}_e$ and $\hat{\mathcal{I}}_{co}$) and those in configuration space (i.e., \mathcal{I}_w). Note that in the particle balance of all electrons, the term due to time varying Φ (i.e., \mathcal{I}_Φ) does not appear since such variation cannot modify the total number of electrons.

C. Description of the ions

In order to calculate the ambipolar and wall potentials, one needs to describe the ions (recall that only positive ions are treated here). Generally, the description of the ions is straightforward by solving a relatively simple ion continuity equation. This equation can be approximated by an ambipolar diffusion equation in a collision-dominated regime. For the present purposes, a treatment describing only the general trends of ion behavior is sufficient. Hence, we assume that the ion density profile does not change in time and the decay of its volume-averaged value $\langle n_i \rangle$ is simply described by $d\langle n_i \rangle/dt = -\langle n_i \rangle/\tau_{amb}$, where $\tau_{amb} = \Lambda^2/D_{amb}$, $D_{amb} = D_i(1 + 2\langle W_e \rangle/3T_a)$, D_i is the ion diffusion coefficient, and T_a the atom (gas) temperature. This gives the time-space evolution of the ion density as

$$n_i(t, r) = n_i(t=0, r) \exp\left[-\int_0^t dt' / \tau_{amb}(t')\right]. \quad (14)$$

D. Calculation of the ambipolar and wall potentials

Having derived the model equations for the ions and the particle-balance equations for the electrons, one can find the ambipolar potential Φ in the plasma and the potential jump

in the wall sheath $\Delta\Phi_w$ or the total wall potential Φ_w . Now, Φ can be found from Eq. (8) with a known $n_i(r) = n_e[\Phi(r)]$ and given EDF $f_0(\epsilon)$. In order to find Φ_w , one can take into account that $d\langle n_e \rangle/dt = d\langle n_i \rangle/dt = -2\Gamma_{iw}/R$, with Γ_{iw} being the ion flux at the wall. This gives, using Eq. (13),

$$\mathcal{I}_w = 2\Gamma_{iw}/R. \quad (15)$$

This equation will be used in our numerical scheme to calculate Φ_w (see Sec. III). Alternatively, as mentioned in Sec. II B, Φ_w can be found from the particle balance of trapped electrons in Eq. (10). In what follows, we shall find an approximate expression for Φ_w using that equation.

It turns out that, under conditions of strong departure from quasistationarity ($\nu_e \rightarrow 0$) and fast removal of free electrons to the wall ($\tau_w \rightarrow 0$), it is possible to derive a simple expression for Φ_w , which closely approximates the numerical results. Under these circumstances, the EDF of trapped electrons experiences no energy relaxation, i.e., $f_0(t, \epsilon) = f_0(t=0, \epsilon)$ for $\epsilon \leq e\Phi_w$, and that of free electrons is zero, i.e., $f_0(t, \epsilon) = 0$ for $\epsilon > e\Phi_w$. Then, with $\hat{\mathcal{I}}_{co} \gg \hat{\mathcal{I}}_e, \hat{\mathcal{I}}_\Phi$ (the cutoff mechanism is dominant), the particle balance of trapped electrons in Eq. (10), together with $d\langle \hat{n}_e \rangle/dt \approx -2\Gamma_{iw}/R$, gives

$$-\overline{\sqrt{w}f_0}|_{\epsilon=e\Phi_w} \frac{de\Phi_w}{dt} \approx 2\Gamma_{iw}/R. \quad (16)$$

This equation simply states that the electron flux to the wall is formed by electrons cut off from the bulk EDF and it can be solved for a given EDF $f_0(\epsilon)$. Then assuming, for simplicity, the initially Maxwellian EDF of Eq. (9) for *trapped electrons*, this equation yields

$$\Phi_w \approx -T_e/e \ln(C + t/\tau_{co}), \quad (17)$$

where $C = \exp(-e\Phi_{w0}/T_e)$ and $\tau_{co} = \tau_{amb} \sqrt{e\Phi_{w0}/T_e}$ with $e\Phi_{w0} = e\Phi_w(t=0)$.

This expression for Φ_w can then be contrasted with the familiar expression for $\Phi_w = \Delta\Phi_w + \Phi(R) \approx \Delta\Phi_w$ (with $|\Phi(R)| \ll |\Delta\Phi_w|$), where

$$\Delta\Phi_w = T_e/2e \ln(M/2\pi m), \quad (18)$$

obtained assuming a Maxwellian EDF for *all electrons* and Bohm’s ion flux at the wall [17]. The ‘‘Maxwellian’’ expression for $\Phi_w \approx \Delta\Phi_w$ in Eq. (18) ($\Delta\Phi_w \approx 4.7T_e/e$ for Ar), being qualitatively different from that in Eq. (17), will be seen to reproduce the numerical results incorrectly (see Sec. IV).

The condition of fast removal of free electrons to the wall (i.e., $\tau_w \rightarrow 0$) used to obtain Eq. (17) can be relaxed by taking into account a finite τ_w . This gives (for $\nu_e \rightarrow 0$) an improved expression for the EDF,

$$f_0(t, \epsilon) = f_0(t=0, \epsilon) \exp\left[-\int_0^t dt' / \tau_w(t', \epsilon)\right] \quad (19)$$

[where $\tau_w^{-1} = 0$ for $\epsilon \leq e\Phi_w(t)$], that can then be used to find Φ_w and be compared with numerical results. (Note that in

the case where e - a inelastic collisions are important the substitution $\tau_w^{-1} \rightarrow \tau_w^{-1} + \nu^*$ allows them to be accounted for.)

III. NUMERICAL SCHEME

The present problem was solved on the radius–total-energy grid. The nonlocal kinetic equation (2) was finite differenced on the total-energy grid and on the radial grid neither finite differentiation nor boundary conditions needed to be applied because of the approximate ion-diffusion model (see Sec. II C). Radial spatial resolution was important, however, since the evolution of the ambipolar potential profile $\Phi(r)$ was self-consistently calculated on the radial grid and was found to be rather critical for predicting correctly such parameters as Φ_w . Due to the importance of the nonlinear e - e collision operator, its careful treatment is essential. Such a treatment must ensure that the finite-differenced e - e operator satisfies the three basic conditions, namely, the conditions of conservation of density and mean total energy and the condition of convergence toward a Maxwellian EDF. The finite-difference discretization method for the e - e collision operator in total-energy formulation was therefore developed as detailed in the Appendix. In order to solve the time-dependent kinetic equation (2), we used a simple, first-order time-advance scheme. The e - e collision operator was implicitly inverted (in principle an unconditionally stable scheme) and the finite-difference discretization method allowed relatively large time steps $\Delta t \sim \nu_e^{-1}(\epsilon_{\min})$, so that the scheme was stable and the relative contribution of the e - e term in the energy balance of all electrons was smaller than 10^{-3} for typical time steps of $\leq 0.1 \mu\text{s}$. (This contribution, which tends to zero as $\Delta t \rightarrow 0$, can hence be identified as a residual error.) Also implicitly treated was the second term on the lhs of the kinetic equation (2).

The general numerical scheme was as follows. Starting with some initial $f_0(\epsilon)$ and $n_i(r)$, first, the EDF f_0 in Eq. (2) is advanced in time, then the ambipolar potential $\Phi(r)$ is found from Eq. (8) with a given $n_i(r)$ and $f_0(\epsilon)$ and the wall potential Φ_w from Eq. (15), and finally the (approximate) ion-diffusion equation (14) is advanced to obtain $n_i(r)$. This procedure is then repeated to advance further in time. Both radial and total-energy grids were equidistant and typically 50 radial and 200 total-energy points were used. The use of an equidistant total-energy grid ($\omega_i = \text{const}$, see the Appendix) allows one to avoid the explicit dependence of the discretization coefficients on T_e [see Eq. (A3)]; however, at low mean energies (i.e., in a late afterglow), a grid with an increasing number of points toward low energies may be numerically more advantageous. A typical simulation of $\sim 50 \mu\text{s}$ into the afterglow took about 10 min on a moderate-performance workstation.

It should be mentioned that the present time-advance scheme was found to result in somewhat noisy time derivatives $d\Phi_w/dt$ (and also related quantities, such as $\hat{\mathcal{I}}_{\text{co}}$, $\hat{\mathcal{I}}_{\Phi}$, $\hat{\mathcal{H}}_{\text{co}}$, $\hat{\mathcal{H}}_{\Phi}$) over one time step $\Delta t (\leq 0.1 \mu\text{s})$. This was not a significant problem since over longer time intervals this dependence was found to be rather smooth (recall that the time scale of Φ_w variation $\gg \Delta t$). However, a more elaborate nu-

merical scheme may be considered in order to reduce numerical noise and speed up calculations, such as one employing a higher-order Runge-Kutta scheme for stepping in time and subcycling (updating the ion and ambipolar potential profiles less frequently than the EDF). For the present purposes, however, the scheme employed proved to be adequate.

Finally, we mention the following on the method of solution of the nonlocal kinetic equation with the nonlinear e - e collision operator (see also Ref. [18] for an approximate method of inclusion of this operator in steady-state calculations). Due to the presence of this operator and the importance of e - e collisions, small time steps need to be used [$\Delta t \sim \nu_e^{-1}(\epsilon_{\min})$], higher electron densities and lower energies requiring smaller Δt . As such, simulations of a late afterglow ($t \gg \tau_{\text{amb}}$) can necessitate long computer times. Such simulations can be carried out by using the semianalytic method proposed in Ref. [5], which is based on the assumption of the EDF quasistationarity. To tackle this problem within the framework of the present approach (solving the time-dependent nonlocal kinetic equation), it is possible to simplify the e - e collision operator by writing it in a linear form that depends parametrically on the mean energy (or T_e). This mean energy can then be found from the condition that the energy balance (12) is satisfied at each time step (recall that a linear e - e collision operator does not conserve energy). This method can be applied when the EDF at low energies is close to a Maxwellian and its advantage is that it allows long time steps, which can dramatically reduce the computation time. Such a method represents an analog of the method developed in Ref. [5] (coupling the nonlocal kinetic equation with the energy-balance equation) for a quasistationary plasma, and its implementation and testing are underway, on which a separate report is envisaged.

IV. SIMULATION RESULTS AND DISCUSSION

We considered two cases and chose p and R such that in both cases the initial $\tau_{\text{amb}} (\propto pR^2)$ is about $50 \mu\text{s}$ and a collision-dominated regime ($\lambda \leq R$) is realized for electrons. In case 1, $R = 5 \text{ cm}$ and $p = 50 \text{ mTorr}$ and in case 2, $R = 15 \text{ cm}$ and $p = 5 \text{ mTorr}$, both at room temperature, $T_a = 300 \text{ K}$. These cases will be compared and contrasted. Case 1 is typical for a CCP (with an electrode separation of $\sim 7 \text{ cm}$, e.g., [10]; see also Ref. [4]). Case 2 is typical for an ICP in which the plasma reactor is relatively large and the gas pressure is low (e.g., [1,8]). It is clear that experimental geometry is never purely cylindrical, but the main phenomena can be expected to be captured for geometries other than cylindrical with similar characteristic dimensions Λ (recall that the nonlocal kinetic equation does not depend explicitly on geometry). The collision cross sections required were taken as in Ref. [9] and $D_i = 40/p \text{ cm}^2/\text{s}$ was used (with p in Torr). It is evident that at a given pressure and geometry the studied mechanisms will be more pronounced for low $\nu_e(e\Phi_w)$, which corresponds to relatively moderate electron densities ($n_e \leq 5 \times 10^{10} \text{ cm}^{-3}$) and/or large electron energies ($T_e \geq 3 \text{ eV}$). We considered here moderate n_e , namely, $n_{e0}(t=0) = 5 \times 10^9 \text{ cm}^{-3}$ in case 1 and 10^{10} cm^{-3} in case 2; this

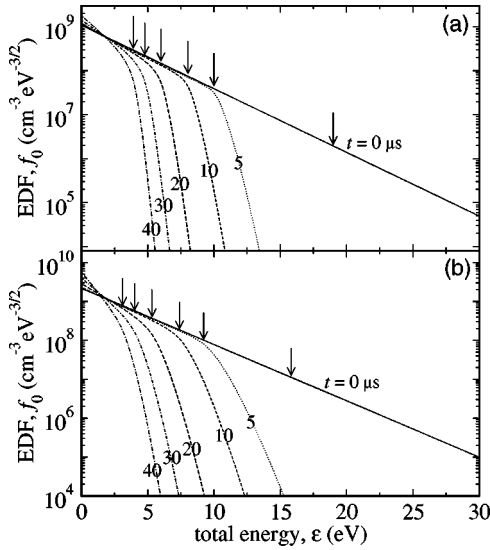


FIG. 1. EDF's $f_0(t, \epsilon)$ at different instants t in the afterglow: (a) case 1 and (b) case 2. The arrows indicate the values of the wall potential energy $\epsilon = e\Phi_w$.

corresponds to $\langle \nu_e(e\Phi_{w0}) \rangle^{-1} \sim 200 \mu\text{s}$ and $100 \mu\text{s}$, respectively (where Φ_{w0} is the initial wall potential). The initial ion density profile $n_i(t=0, r)$ [see Eq. (14); recall that $n_i = n_e$] was chosen to be parabolic with the boundary-to-central density ratio of $1/3$. In order to separate the studied mechanisms from other possible effects, the initial EDF $f_0(t=0, \epsilon)$ was chosen to be the Maxwell-Boltzmann $f_M(\epsilon)$ of Eq. (9) with $T_e = 3 \text{ eV}$ (i.e., the initial $W_e = 4.5 \text{ eV}$ and is spatially uniform). A distribution close to a Maxwellian (at least at low energies) can be observed during the power-on period in both an ICP and a CCP. Since the complete $e-e$ collision operator was included in the calculations, the evolution of any other initial EDF can be treated appropriately, together with mechanisms such as Maxwellization. Simulations were carried out over the first $50 \mu\text{s}$ into the afterglow during which the mean energy of electrons decreases by a factor of 4–6.

We start by presenting in Fig. 1 the EDF's $f_0(t, \epsilon)$ at different moments t into the afterglow (including the initial Maxwellian EDF) for the two cases studied. One can see that in both cases, during the first $5 \mu\text{s}$, the high-energy tail of the EDF (corresponding to free electrons) falls off dramatically, the wall potential energy $e\Phi_w$ (indicated by arrows) decreasing by a factor of 2 (see also Fig. 2 below). At later times ($t \geq 5 \mu\text{s}$), a slower evolution of the EDF with time takes place. An important feature is that the overall EDF quickly becomes non-Maxwellian and remains so even at later times when the mean kinetic energy has decreased significantly (up to six times; see Figs. 4 and 5 below). Moreover, for $t \leq 30 \mu\text{s}$ in case 1 and $t \leq 20 \mu\text{s}$ in case 2, the EDF of trapped electrons ($\epsilon \leq e\Phi_w$) shows little variation with time (i.e., it remains closely Maxwellian with $T_e = 3 \text{ eV}$), which suggests that at these times the EDF does have time to respond to changes in the electric potential/field and thus a strong departure from quasistationarity occurs. At later times, the EDF of trapped electrons starts to deviate from the initial distri-

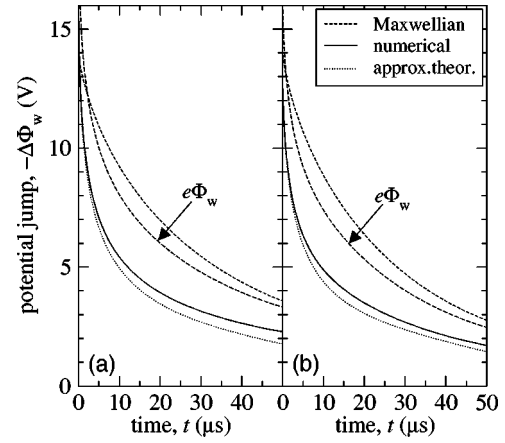


FIG. 2. Time evolution of the sheath potential jump $\Delta\Phi_w$: (a) case 1 and (b) case 2. The solid lines correspond to the numerical results, the dotted lines are calculations according to the approximate theoretical estimate in Eq. (17), and the dashed lines are calculations using expression (18) (assumption of a Maxwellian EDF). Also shown are the time evolutions of the wall potential $e\Phi_w$ (long-dashed lines).

bution, its low-energy part being driven Maxwellian (with lower T_e 's) by $e-e$ collisions. Another important feature concerns the EDF of free electrons. One can see that, in case 1 [see Fig. 1(a)], this EDF falls with increasing energy markedly faster than in case 2 [see Fig. 1(b)]. Clearly, this behavior is determined by the rate of escape to the wall, namely, by τ_w in Eq. (1), which in turn has two contributions. The first term in τ_w , which defines the free-diffusion time, is proportional to pR^2 and so is approximately the same in case 1 and case 2. Although the regime is (nearly) collision dominated, the second term, which defines the free-flight escape time (approximately $\propto p^{-1}$), comes into play in case 2 because of the lower pressure. Therefore, τ_w is larger in case 2 than in case 1, i.e., free electrons escape to the wall more quickly in case 1 than in case 2. This fact has important consequences on the density and energy balances of trapped electrons (see discussion of Figs. 4 and 5 below).

The time evolution of the sheath potential jump $\Delta\Phi_w$ as predicted by the simulations is plotted in Fig. 2 for the two cases studied and the corresponding time-space evolution of the ambipolar potential Φ is shown in Fig. 3. One can see in Fig. 2 that $|\Delta\Phi_w|$ decreases quickly during the first $10 \mu\text{s}$, and later on the decrease rate is slower. In contrast, inspection of Fig. 3 reveals that the ambipolar potential evolves slowly with time, which is consistent with the slow evolution of the mean electron energy. Also plotted in Fig. 2 is the ‘‘Maxwellian’’ $\Delta\Phi_w$ according to Eq. (18) using the numerical $T_e = \frac{2}{3}\langle W_e \rangle$. One can see that, even though the Maxwellian and numerical $\Delta\Phi_w$ are close at the initial moment $t = 0$ (at which the EDF is taken to be Maxwellian), throughout most of the simulation period the Maxwellian $|\Delta\Phi_w|$ is larger than the numerical one by about a factor of 2. (Note that the ‘‘ T_e ’’ used here represents the mean energy of electrons; taking ‘‘ T_e ’’ as the slope of the Maxwellian part of the EDF will result in even larger disagreement because such ‘‘ T_e ’’ remains nearly unchanged for $t \leq 20\text{--}30 \mu\text{s}$; see Fig.

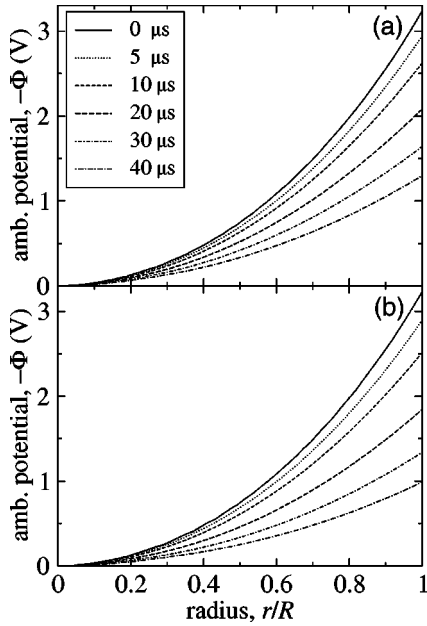


FIG. 3. Ambipolar-potential radial profiles at different instants t in the afterglow: (a) case 1 and (b) case 2.

1.) The fact that Eq. (18) significantly overestimates $|\Delta\Phi_w|$ is common (see also Ref. [5]), and it can lead to a significant overestimation of the energy of ions impinging on the wall surface and also of the rate of diffusion cooling ($\propto e\Phi_w$). By contrast, the approximate theoretical estimate of $\Delta\Phi_w$ according to Eq. (17) [using numerical $\Phi(t, R)$] is seen to be very close to the numerical results (see Fig. 2); deviations take place when the EDF of trapped electrons starts to deviate from the initial distribution ($t \gtrsim 20\text{--}30 \mu\text{s}$; see Fig. 1). Also, calculations using the EDF $f_0(t, \epsilon)$ of Eq. (19) instead of that calculated from the kinetic equation (2) showed good agreement with the numerical results for $t \lesssim 20\text{--}30 \mu\text{s}$.

The time evolutions of different contributions in the density and energy balances of trapped electrons [see Eqs. (10) and (12)] are plotted in Fig. 4 for case 1 and in Fig. 5 for case 2. Also plotted are the time evolutions of the volume-averaged density $\langle n_e \rangle$ and mean kinetic energy $\langle W_e \rangle$. One can see that $\langle n_e \rangle$ decreases with time by a factor of ~ 2 in both cases, whereas $\langle W_e \rangle$ decreases by a factor of ~ 4 in case 1 and ~ 6 in case 2. An important observation is that the initial decrease of $\langle W_e \rangle$ at $t \lesssim 20\text{--}30 \mu\text{s}$ takes place at an almost unperturbed EDF of trapped electrons (in particular, the EDF slope, or the ‘‘Maxwellian’’ T_e , does not change; see Fig. 1), which implies the significance of the cutoff mechanism. The spatial profile of the mean (kinetic) energy of electrons, $W_e(r)$, is nearly parabolic throughout the simulation period with the central-to-boundary ratio increasing from 1 at $t=0$ up to ~ 1.4 at $t \sim 20\text{--}30 \mu\text{s}$ and then slowly decreasing. [Recall that in these calculations the ion density profile is assumed to be parabolic with its volume-averaged value being calculated; see Eq. (14) and Figs. 4 and 5.]

As far as the balance equations are concerned the following can be observed. One can see in Fig. 4(a) that in case 1 during the first $20 \mu\text{s}$ the particle loss of trapped electrons is dominated by the cutoff mechanism (i.e., $\hat{\mathcal{I}}_{\text{co}} > \hat{\mathcal{I}}_e$); at later

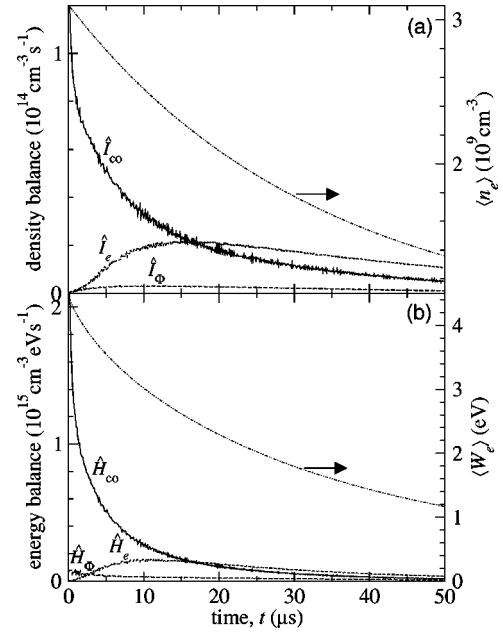


FIG. 4. Time evolution of different contributions in the density (a) and energy (b) balances of trapped electrons [see Eqs. (10) and (12)] in case 1: $\hat{\mathcal{I}}_{\text{co}}$ and $\hat{\mathcal{H}}_{\text{co}}$ (solid lines); $\hat{\mathcal{I}}_e$ and $\hat{\mathcal{H}}_e$ (short-dashed lines); $\hat{\mathcal{I}}_\phi$ and $\hat{\mathcal{H}}_\phi$ (dashed lines). Also plotted on the rhs axes are the time evolutions of the volume-averaged density $\langle n_e \rangle$ (a) and mean kinetic energy $\langle W_e \rangle$ (b).

times, particle losses due to $e\text{--}e$ collisions become more significant. The same can be said regarding the energy balance [see Fig. 4(b)]. One can note the unimportance of the $\hat{\mathcal{I}}_\phi$ and $\hat{\mathcal{H}}_\phi$ terms in both case 1 and case 2 [see Figs. 4 and 5]. As expected, in both cases studied, cooling in collisions with free electrons (term $\hat{\mathcal{H}}_f$, not plotted in Figs. 4 and 5) is negligible, being smaller by at least a factor of 10 compared

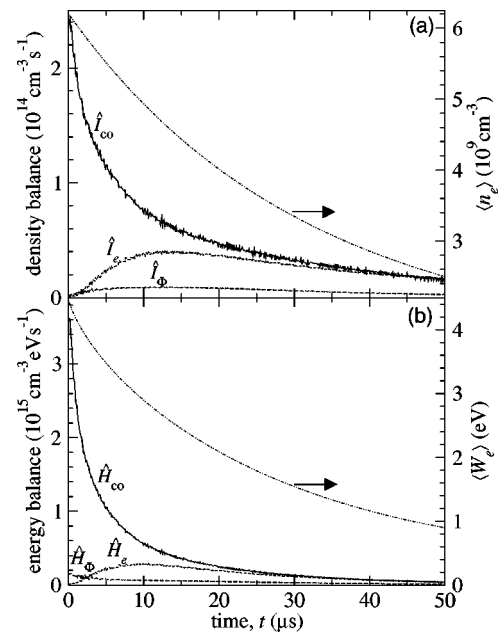


FIG. 5. Same as Fig. 4, but for case 2.

with the other mechanisms. In contrast to case 1, in case 2 (see Fig. 5), the cutoff mechanism is more important throughout most of the simulation period in both the particle and energy balances (i.e., $\hat{\mathcal{I}}_{\text{co}} > \hat{\mathcal{I}}_e$ and $\hat{\mathcal{H}}_{\text{co}} > \hat{\mathcal{H}}_e$) even though the electron density is higher in case 2 than in case 1 (and τ_{amb} 's are almost the same). Two factors may contribute to this. First, since the removal rate to the wall is lower (τ_w is larger) in case 2 than in case 1 (see discussion of Fig. 1), the EDF at $\epsilon = e\Phi_w$ (and hence $\hat{\mathcal{I}}_{\text{co}}$ and $\hat{\mathcal{H}}_{\text{co}}$) is larger and its slope (hence $\hat{\mathcal{I}}_e$ and $\hat{\mathcal{H}}_e$) is smaller in case 2 than in case 1. Second, the higher electron density in case 2 may result in stronger Maxwellization and hence in lower $\hat{\mathcal{I}}_e$ and $\hat{\mathcal{H}}_e$ (recall that for a purely Maxwellian EDF $\hat{\mathcal{I}}_e = \hat{\mathcal{H}}_e = 0$). Accordingly, one can observe (see Fig. 5) that the rates $\hat{\mathcal{I}}_e$ and $\hat{\mathcal{H}}_e$ decrease with time for $t \geq 10\text{--}15 \mu\text{s}$. These facts suggest that, without solving the complete problem, it would be difficult to predict beforehand whether or not the cutoff mechanism will be important for a given set of plasma conditions. Only as a first approximation, its importance can be expected when $\nu_e(e\Phi_w) < \tau_{\text{amb}}^{-1}$.

Let us now briefly discuss the possible impact of quasi-elastic and inelastic e - a collisions. It is clear that, as far as the particle balance of trapped electrons is concerned, such collisions prevent electrons from escaping from the potential well, generating particle inflows (negative fluxes). Thus, provided that e - a collisions are frequent and e - e collisions are rare at high energies, the cutoff mechanism has to provide large particle outflows, which overcome the inflows generated in e - a collisions. The presence of e - a collisions, therefore, can in fact *enhance* the cutoff mechanism. In a noble gas (such as Ar) at low pressures, quasi-elastic collisions are generally negligible, whereas inelastic collisions can be important only when the wall potential energy $e\Phi_w$ greatly exceeds the threshold of inelastic collisions w^* . It is then likely that such types of collisions can be more important in a molecular gas, in which they are often approximated as quasi-elastic with a characteristic frequency $\delta_m \nu_m$. When $\delta_m \nu_m > \nu_e$ at high energies, the situation can be quite different from that in a noble gas. Indeed, due to the high frequency of electron-molecule collisions $\delta_m \nu_m$, the EDF can be *quasistationary* (but nonlocal, such that $\lambda_\epsilon \approx \lambda \sqrt{\nu/\delta_m \nu_m} > \Lambda$), and the cutoff mechanism will still have to provide the necessary particle outflows until $e\Phi_w$ drops to a value low enough so that $\nu_e \geq \delta_m \nu_m$ at $\epsilon \sim e\Phi_w$. These interesting phenomena in molecular gases will be explored in future work.

Finally, we say a few words on comparison with experiment. Comprehensive probe measurements of the EDF and of the plasma potential ($\sim \Phi_w$) are necessary over the first 50–100 μs into the afterglow in order to be able to identify the mechanisms predicted here. Such measurements could not be found in the literature. Generally, the electron temperature is found from logarithmic slopes of probe V - I characteristics at low energies. Obviously, such an ‘‘electron temperature’’ describes only the Maxwellian part of the EDF, which is likely to be non-Maxwellian at higher energies in a low-pressure afterglow plasma.

V. SUMMARY AND CONCLUSIONS

In this paper, we develop a model for self-consistent kinetic description of a low-pressure afterglow plasma. The model is applied to simulate the transient phenomena taking place under conditions where the EDF is not quasistationary. In particular, a cutoff mechanism is brought forward and shown to be important for the particle and energy balances of trapped electrons. This mechanism is essential for predicting correctly the self-consistent wall potential and the rate of diffusion cooling. The time-dependent nonlocal kinetic equation is solved and the e - e collision operator is taken into account by extending Rockwood's discretization scheme in total-energy formulation. Strongly non-Maxwellian EDF's are predicted and it is observed that, depending on plasma conditions, the transient period may be rather long, of order of the ambipolar diffusion time, lower pressures resulting in longer transient times. A method is suggested for possible speeding up of the calculation under conditions of strong e - e interaction at low (thermal) energies. It is likely that the studied phenomena manifest themselves in molecular gases, even when the EDF is quasistationary. The cutoff mechanism may also be important in a high-density electronegative plasma where the electron density is low (i.e., lower than the ion density) during the power-on period and an ion-ion plasma can form during the power-off (afterglow) period [19]. This is because the presence of negative ions requires a higher rate of electron loss than in an electropositive plasma, this process becoming increasingly more important as the plasma decays. Since there is increasing evidence of the effectiveness of the nonlocal approach for various types of steady-state plasmas at low pressures (e.g., [8–10]), it is possible to extent the proposed method for self-consistent kinetic modeling of low-pressure pulsed plasmas during both the power-on and power-off periods, including the breakdown period. An extension to multidimensional geometry can also be made (e.g., [8]).

APPENDIX: FINITE-DIFFERENCE REPRESENTATION OF THE e - e COLLISION OPERATOR

The method of discretization of the e - e collision operator in kinetic energy formulation was proposed by Rockwood [20] and extended in Ref. [21] for a nonequidistant energy mesh. Here we develop the corresponding scheme for the e - e collision operator in total-energy formulation [given by Eqs. (5) and (6)] by following the notation and methodology of Ref. [21]. We define the total-energy grid as $(\epsilon_1, \epsilon_2, \dots, \epsilon_N)$ with $b_j = \epsilon_j + \frac{1}{2}\omega_j$ and $b_{j-1} = \epsilon_j - \frac{1}{2}\omega_j$ being the upper and lower bounds of the interval centered at ϵ_j with $j \in [1, N]$. The flux derivatives at $\epsilon = \epsilon_j$ are calculated as $\partial \mathcal{J}_{ee} / \partial \epsilon = [\mathcal{J}_{ee}(b_j) - \mathcal{J}_{ee}(b_{j-1})] / \omega_j$, where the flux itself at $\epsilon = b_j$ is represented as $\mathcal{J}_{ee}(b_j) = -\alpha_j f_0(\epsilon_j) + \beta_{j+1} f_0(\epsilon_{j+1})$. The integrals in Eq. (6) are represented as sums, which gives

$$\alpha_j = \sum_k A_{jk} f_0(\epsilon_k) \quad \text{and} \quad \beta_j = \sum_k B_{jk} f_0(\epsilon_k). \quad (\text{A1})$$

The three basic conditions that the e - e collision operator must satisfy are used in order to establish the relationship between the matrices A and B and between the elements of these matrices themselves. The conditions of density and mean total-energy conservation [see Eq. (7)] require that, respectively, $A_{Nl} = B_{1l} = 0$ for any $l \in [1, N]$ and

$$(\epsilon_{j+1} - \epsilon_j)A_{jk} = (\epsilon_k - \epsilon_{k-1})B_{kj}, \quad (\text{A2})$$

and the third condition of convergence toward a Maxwellian distribution [$\propto \exp(-\epsilon/T_e)$] implies

$$A_{jk} = \frac{\epsilon_k - \epsilon_{k-1}}{\epsilon_{j+1} - \epsilon_j} \exp\left(\frac{(\epsilon_k - \epsilon_{k-1}) - (\epsilon_{j+1} - \epsilon_j)}{T_e}\right) A_{k-1j+1}. \quad (\text{A3})$$

The coefficients A_{jk} are then calculated using the same approximations as in Ref. [21]: a function f and its total-energy derivative at $\epsilon = b_l$ are, respectively, $f(b_l) = [\omega_{l+1}f(\epsilon_l) + \omega_l f(\epsilon_{l+1})]/(\omega_l + \omega_{l+1})$ and $\partial f/\partial \epsilon = [f(\epsilon_{l+1}) - f(\epsilon_l)]/(\epsilon_{l+1} - \epsilon_l)$. This gives

$$A_{jk} = \begin{cases} \nu_{e0} \frac{\omega_k}{\epsilon_{j+1} - \epsilon_j} \left(-\frac{2}{3} \overline{w^{3/2}}(\epsilon_k) + \frac{1}{2} \overline{w^{1/2}}(\epsilon_k) \omega_j \right) & \text{for } j \geq k \\ -\nu_{e0} \frac{2}{3} \overline{w^{3/2}}(b_j) \frac{\omega_k}{\epsilon_{j+1} - \epsilon_j} & \text{for } j < k. \end{cases} \quad (\text{A4a})$$

$$(\text{A4b})$$

Following Ref. [21], Eq. (A4a) is used to define A_{jk} for $j > k$, Eq. (A4b) to define A_{k-1k} , and the rest of A is found from Eq. (A3). The matrix B is then calculated from Eq. (A2).

-
- [1] M. A. Lieberman and S. Ashida, *Plasma Sources Sci. Technol.* **5**, 145 (1996).
 [2] D. P. Lymberopoulos, V. I. Kolobov, and D. J. Economou, *J. Vac. Sci. Technol. A* **16**, 564 (1998).
 [3] R. W. Boswell and D. Vender, *IEEE Trans. Plasma Sci.* **19**, 141 (1991).
 [4] H. B. Smith, *Phys. Plasmas* **5**, 3469 (1998).
 [5] R. R. Arslanbekov and A. A. Kudryavtsev, *Phys. Rev. E* **58**, 7785 (1998).
 [6] I. B. Bernstein and T. Holstein, *Phys. Rev.* **94**, 1475 (1954).
 [7] L. D. Tsendin, *Zh. Èksp. Teor. Fiz.* **66**, 1638 (1974) [*Sov. Phys. JETP* **39**, 805 (1974)].
 [8] V. I. Kolobov and W. N. G. Hitchon, *Phys. Rev. E* **52**, 972 (1995).
 [9] U. Kortshagen, G. J. Parker, and J. E. Lawler, *Phys. Rev. E* **54**, 6746 (1996).
 [10] S. V. Berezhnoi, I. D. Kaganovich, and L. D. Tsendin, *Plasma Sources Sci. Technol.* **7**, 268 (1998).
 [11] L. D. Tsendin, *Plasma Sources Sci. Technol.* **4**, 200 (1995).
 [12] U. Kortshagen, C. Busch, and L. D. Tsendin, *Plasma Sources Sci. Technol.* **5**, 1 (1996).
 [13] L. D. Tsendin and Y. B. Golubovskii, *Zh. Tekh. Fiz.* **47**, 1839 (1977) [*Sov. Phys. Tech. Phys.* **22**, 1066 (1977)].
 [14] L. D. Tsendin, *Fiz. Plasmy* **8**, 169 (1982) [*Sov. J. Plasma Phys.* **8**, 96 (1982)].
 [15] R. R. Arslanbekov and A. A. Kudryavtsev, *Phys. Rev. E* **58**, 6539 (1998); *Phys. Plasmas* **6**, 1003 (1999).
 [16] N. B. Kolokolov, A. A. Kudryavtsev, and O. G. Toronov, *Zh. Tekh. Fiz.* **55**, 1920 (1985) [*Sov. Phys. Tech. Phys.* **30**, 1128 (1985)].
 [17] M. A. Lieberman and A. J. Lichtenberg, *Principles of Plasma Discharges and Materials Processing* (Wiley, New York, 1994).
 [18] D. Uhrlandt, M. Schmidt, and R. Winkler, *Comput. Phys. Commun.* **118**, 185 (1999).
 [19] S. A. Gutsev, A. A. Kudryavtsev, and V. A. Romanenko, *Zh. Tekh. Fiz.* **65**, 77 (1995) [*Tech. Phys.* **40**, 1131 (1995)].
 [20] S. D. Rockwood, *Phys. Rev. A* **8**, 2348 (1973).
 [21] J. Bretagne, J. Godart, and V. Puech, *J. Phys. D* **15**, 2205 (1982).